

A Fast Hydrogen Sulfide-Releasing Donor Increases the Tumor Response to Radiotherapy

Géraldine De Preter¹, Caroline Deriemaeker¹, Pierre Danhier¹, Lucie Brisson², Thanh Trang Cao Pham¹, Vincent Grégoire³, Bénédicte F. Jordan¹, Pierre Sonveaux², and Bernard Gallez¹

Abstract

Hydrogen sulfide (H₂S) is the last gaseous transmitter identified in mammals, and previous studies have reported disparate conclusions regarding the implication of H₂S in cancer progression. In the present study, we hypothesized that sodium hydrosulfide (NaHS), a fast H₂S-releasing donor, might interfere with the mitochondrial respiratory chain of tumor cells, increase tumor oxygenation, and potentiate the response to irradiation. Using electron paramagnetic resonance (EPR) oximetry, we found a rapid increase in tumor pO₂ after NaHS administration (0.1 mmol/kg) in two human tumor models (breast MDA-MB-231 and cervix SiHa), an effect that was due to a decreased oxygen consumption and an increased tumor perfusion. Tumors irradiated 15 minutes after a single NaHS administration were more sensitive to irradiation compared with those that received

irradiation alone (increase in growth delay by 50%). This radiosensitization was due to the oxygen effect, as the increased growth delay was abolished when temporarily clamped tumors were irradiated. In contrast, daily NaHS injection (0.1 mmol/kg/day for 14 days) did not provide any effect on tumor growth *in vivo*. To understand these paradoxical data, we analyzed the impact of external factors on the cellular response to NaHS. We found that extracellular pH had a dramatic effect on the cell response to NaHS, as the proliferation rate (measured *in vitro* by BrdU incorporation) was increased at pH = 7.4, but decreased at pH = 6.5. Overall, our study highlights the complex role of environmental components in the response of cancer cells to H₂S and suggests a new approach for the use of H₂S donors in combination with radiotherapy. *Mol Cancer Ther*; 15(1); 154–61. ©2015 AACR.

Introduction

Hydrogen sulfide (H₂S) has emerged as an important endogenous modulator and is now considered the third member of the gasotransmitter family, along with nitric oxide (NO) and carbon monoxide (CO; ref. 1). H₂S is an enzymatically produced small molecule that can freely cross biologic membranes and exert a wide range of actions. H₂S most known effect is the reversible inhibition of the last mitochondrial electron acceptor, cytochrome C oxidase (2). Other H₂S targets have been reported so that H₂S appears also implicated in the cardiovascular system. H₂S dilates rat and human blood vessels by opening smooth muscle cells K_{atp} channels (3). Other cardiovascular effects of H₂S, such as protection against ischemia/reperfusion injury, have been described (4). Moreover, H₂S

effects are also found in the nervous and endocrine systems, as well as in inflammation (5). Since the discovery that H₂S is important for physiologic and pathologic processes, development and clinical applications of injectable donors allowing controlled and safe administration of the molecule have attracted growing interest (6). Because of their commercial availability, preclinical and clinical studies have been conducted using fast H₂S-releasing inorganic salts, such as sodium hydrosulfide (NaHS) and sodium sulfide (Na₂S; ref. 7).

Until now, investigations in cancer research have mainly focused on the effects of H₂S on proliferation and survival of cancer cells (8–11). However, controversial results exist, as evidenced by the reported increased (8) or decreased (9) proliferation of colon cancer cells following NaHS treatment. A study showed that H₂S derived from NaHS may confer intrinsic radioresistant properties to cancer cells (12). However, the beneficial effects of H₂S as cotreatment to radiotherapy have never been studied *in vivo*. We paid attention to this latter aspect because it was previously shown that NO, another gaseous mediator, radiosensitizes tumors in mice (13–15). It was shown that NO acts as an intrinsic radiosensitizer but also acts through an "oxygen enhancement" effect, alleviating tumor hypoxia, which is a major cause of resistance to radiotherapy (16, 17). pO₂ values of 2.5 mmHg or less are characteristic of advanced solid tumors in a wide range of human cancers (18), and oxygen tensions below 10 mmHg are estimated to significantly reduce radiosensitivity (19). It is related to the fact that oxygen enhances water radiolysis and fixes DNA damage following radiation treatment.

¹Biomedical Magnetic Resonance Research Group, Louvain Drug Research Institute (LDRI), Université catholique de Louvain, Brussels, Belgium. ²Pole of Pharmacology and Therapeutics, Institute of Experimental and Clinical Research (IREC), Université catholique de Louvain, Brussels, Belgium. ³Pole of Molecular Imaging, Radiotherapy and Oncology, Institute of Experimental and Clinical Research (IREC), Université catholique de Louvain, Brussels, Belgium.

Note: Supplementary data for this article are available at Molecular Cancer Therapeutics Online (<http://mct.aacrjournals.org/>).

Corresponding Author: Bernard Gallez, Université catholique de Louvain, LDRI-REMA, Avenue Mounier 73.08, B-1200 Brussels, Belgium. Phone: 0032-2-7647391; Fax: 0032-2-7647390; E-mail: bernard.gallez@uclouvain.be

doi: 10.1158/1535-7163.MCT-15-0691-T

©2015 American Association for Cancer Research.

In the present study, we considered the potential effect of NaHS administration on tumor hypoxia and response to irradiation. Considering the origins of tumor hypoxia (18), the effects of NaHS treatment on the delivery of oxygen from the blood and on oxygen consumption by cancer cells were examined. We also investigated *in vitro* and *in vivo* impact of NaHS on cancer cell growth when used as a single therapeutic compound.

Materials and Methods

Cell culture and reagents

The human cervix carcinoma SiHa and the human breast cancer MDA-MB-231 cell lines were from the American Type Culture Collection (ATCC). SiHa cancer cells were obtained in 2012, and MDA-MB-231 cancer cells were obtained in 2011. Cell lines were authenticated by the provider and were frozen in liquid nitrogen soon after arrival. In this study, aliquots were thawed and early passage (<20 passages) cells were used. Cells were grown in DMEM + Glutamax (Life Technologies) containing 4.5 g/L glucose supplemented with 10% heat inactivated FBS and 1% penicillin-streptomycin. For the experiments, culture medium containing no glutamine was used. pH was buffered with 10 mmol/L PIPES or 3.7 g/L sodium bicarbonate. For the oxygen consumption measurements, where no incubation time was used, pH was adjusted to 6.5, 7.0, or 7.5 with HCl 0.1 mol/L and NaOH 0.1 mol/L solutions. All cultures were kept at 37°C in 5% CO₂ atmosphere. NaHS (Sigma) crystals were dissolved in physiologic saline (NaCl 0.9%). Rotenone (Sigma), a mitochondrial complex I inhibitor, was diluted in DMSO. Solutions were freshly prepared before all experiments.

Oxygen consumption rate

The oxygen consumption rate (OCR) of intact whole cells was measured using a Bruker EMX EPR spectrometer operating at 9.5 GHz as previously described (20). Adherent cells were trypsinized and resuspended in fresh medium (10⁷ cells/mL). Hundred μ L of the cell suspension was mixed with 100 μ L of 20% dextran to avoid agglomeration and was sealed in a glass capillary tube in the presence of 0.2 mmol/L of a nitroxide probe acting as an oxygen sensor (¹⁵N 4-oxo-2,2,6,6-tetramethylpiperidine-d₁₆-¹⁵N-1-oxyl, CDN isotopes). Cells were maintained in 37°C during the acquisition of the spectra. EPR linewidth was measured every minute and reported on a calibration curve to obtain the oxygen concentration (13). OCR was determined by the absolute value of the slope of the decrease in oxygen concentration in the closed capillary tube.

Cell proliferation

Cell proliferation was assayed with a 5-bromo-2'-deoxyuridine (BrdU)-ELISA-based method (Roche) following the provider's instructions. Cells were incubated in the presence of BrdU (a nucleotide analogue) during 4 hours, and the amount of BrdU incorporated in the cells was assessed by colorimetric measurements using a plate reader (SpectraMax M2e; Molecular Devices).

Glucose consumption

Extracellular glucose consumption was measured from supernatant of cultured cells. Metabolite concentration was enzymatically quantified on deproteinized samples with a CMA600 ana-

lyzer (CMA Microdialysis AB). Glucose consumption was normalized to protein content using the Pierce BCA Protein assay (Thermo Scientific).

Intracellular ATP quantification

Total intracellular ATP was measured by the ATP Determination Kit (Life Technologies) according to the manufacturer's protocol. Cells were washed twice with PBS and lysed in the buffer recommended by the manufacturer (10 mmol/L Tris, 1 mmol/L EDTA, 100 mmol/L NaCl, 0.01% Triton X-100). Cell lysates were added to a reaction mixture containing luciferase and luciferine for bioluminescence measurements using a plate reader (SpectraMax M2e; Molecular Devices). A standard curve was generated with known ATP concentrations in the same conditions. Intracellular ATP concentration was normalized to protein content using the Pierce BCA Protein assay (Thermo Scientific).

pHi measurements

Cells were incubated for 30 minutes at 37°C in Hank's medium (Sigma) containing 7 μ mol/L 5-(and-6)-Carboxy SNARF-1, Acetoxymethyl Ester, a fluorescent pH indicator (Life Technologies). Cells were washed with Hank's medium, and fluorescence (excitation 485 nm; emission 580 and 642 nm) was detected using a plate reader (SpectraMax i3; Molecular Devices). Fluorescent values were converted into pH values using the nigericin/high K⁺ solution calibration technique according to the manufacturer.

Mouse models and *in vivo* experiments

Five-week-old female NMRI nude mice (Janvier Labs) were intramuscularly injected with 10⁷ SiHa or MDA-MB-231 human cancer cells in the rear leg. Tumor xenografts were allowed to grow up to 8 mm before experimentation. For the treated groups, NaHS was dissolved in physiologic saline (NaCl 0.9%) and given by intraperitoneal injection (100 μ mol/kg body weight). Control animals were treated with physiologic saline only. Animals were anesthetized by inhalation of isoflurane mixed with air (3% induction, 1.8% maintain for a minimum of 15 minutes before any measurement). All animal experiments were conducted in accordance with national animal care regulations.

Tumor oxygenation

EPR oximetry using charcoal (CX 0670-1; EM Sciences) as oxygen sensor was used to dynamically evaluate changes in tumor oxygenation after treatment with NaHS, using a protocol described previously (21). EPR spectra were recorded using an EPR spectrometer (Magnettech), with a low-frequency microwave bridge operating at 1.2 GHz and an extended loop resonator. A suspension of charcoal was injected into the center of the tumor 1 day before measurement (100 mg/mL; 50 μ L injected, particle size of 1–25 μ m). The localized EPR measurements correspond to an average of the pO₂ values in a volume of approximately 10 mm³ (22). For the experiments, baseline values were performed after mice were anesthetized to determine the oxygen status of tumors before injection of the treatment. Then, the effect of NaHS was measured by following tumor pO₂ for 1 hour after the single injection. Body temperature of the mice was kept at 37°C throughout the experiment.

De Preter et al.

Tumor perfusion

The Patent blue staining method was used to obtain an estimation of the tumor perfusion fraction using a protocol described previously (23). Fifteen minutes after NaHS or physiologic saline treatment, 100 μ L of Patent blue (Sigma) solution (1.25%) was injected in the tail vein of the mice. After 1 minute, mice were sacrificed and tumors were excised. To evaluate the tumor perfusion fraction, each tumor was cut into two size-matched halves, and the percentage of stained area of the whole cross-section was determined using an in-house program running on MatLab.

Tumor radioresponse

The tumor was locally irradiated (^{137}Cs γ -irradiator) with a single dose of 16 Gy. Mice were anesthetized, and the tumor was centered in a 3-cm diameter circular irradiation field. Irradiation was given 15 minutes after injection of NaHS or physiologic saline. After radiotherapy, tumor growth was determined using a caliper until the diameter reached 14 mm, time at which the mice were sacrificed.

Statistical analysis

All results are expressed as mean \pm SEM. Differences between groups were analyzed using the unpaired Student *t* test or ANOVA when more than two groups were compared. The value of $P < 0.05$ was considered statistically significant.

Results

NaHS injection increases oxygenation of hypoxic tumors in mice

Hypoxia is a major cause of resistance to radiotherapy in solid tumors. Therefore, we analyzed the capability of the fast H_2S -releasing donor NaHS to increase tumor oxygenation in two human tumor models. As H_2S is rapidly oxidized in biologic samples, local tumor oxygenation was monitored before (baseline) and during 1 hour after intraperitoneal injection of NaHS (100 $\mu\text{mol/kg}$) or vehicle [physiologic saline (NaCl 0.9%)]. Oxygen levels were quantified using EPR oximetry, a sensitive method allowing continuous measurement of pO_2 from the same site over time (21). Our results showed that, as compared with control groups, NaHS injection rapidly increased tumor pO_2 in human breast MDA-MB-231 (Fig. 1A) and human cervix SiHa (Fig. 1B) xenografts, where significant increased oxygenation was observed 15 minutes after NaHS injection. Note the different scales used in Fig. 1A and Fig. 1B. Interestingly, the significant effect on tumor pO_2 correlated with the time to reach maximum plasmatic H_2S concentration following an intraperitoneal injection of NaHS (24).

NaHS inhibits cellular oxygen consumption and enhances tumor perfusion

To understand the significant increase in pO_2 induced by NaHS in hypoxic tumors, oxygen consumption of cancer cells was first studied. We intended to determine *in vitro* how NaHS influences the OCR of MDA-MB-231 and SiHa cancer cells. In aqueous solution, H_2S derived from dissolved NaHS is in equilibrium with the poorly membrane permeant $\text{HS}^- + \text{H}^+$ with a pK_a of 6.9 (25). We therefore analyzed the influence of different extracellular pH (pHe) on OCR inhibition by NaHS.

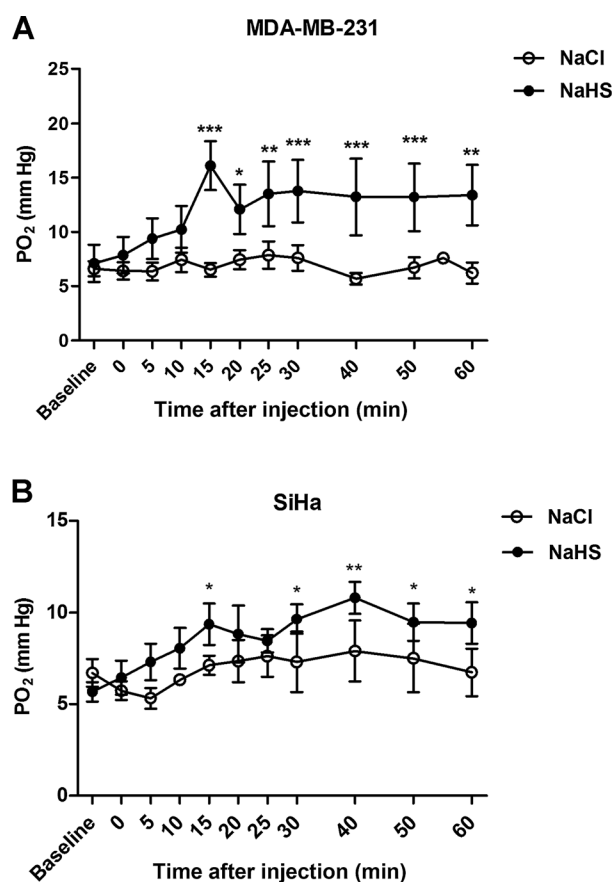
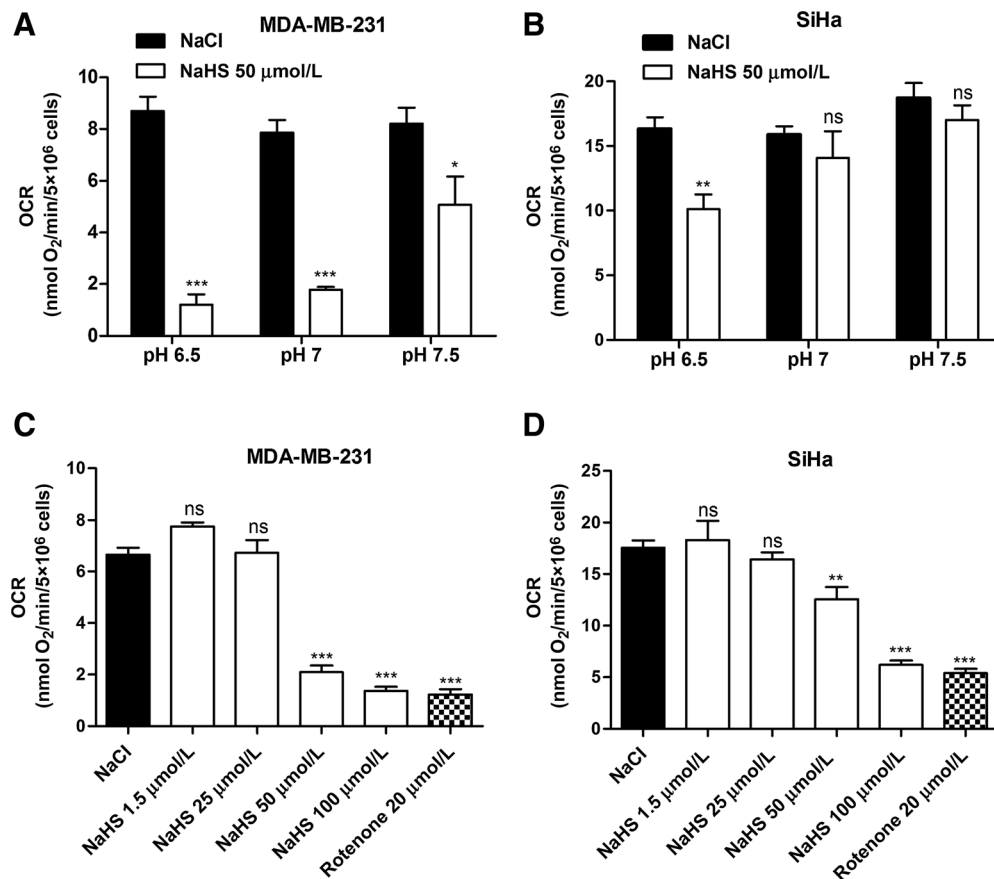


Figure 1. NaHS injection increases tumor pO_2 . Tumor pO_2 was monitored in MDA-MB-231 (A) and SiHa (B) tumors by EPR (L-band) oximetry before (baseline) and after NaHS (100 $\mu\text{mol/kg}$, ●) or vehicle (NaCl 0.9%, ○) i.p. injection (60 minutes). Each point represents mean $\text{pO}_2 \pm$ SEM. *, $P < 0.05$; **, $P < 0.01$; ***, $P < 0.001$. ANOVA and Bonferroni post-test ($n = 5-7/\text{group}$).

As shown in Fig. 2A and B, exposure to 50 $\mu\text{mol/L}$ NaHS instantaneously inhibited OCR in MDA-MB-231 and SiHa tumor cell lines, and the response was dependent on pHe. We observed that OCR inhibition was more effective when pHe decreased. After that to examine the concentration response to NaHS, MDA-MB-231 and SiHa cells were treated with 0, 1.5, 25, 50, and 100 $\mu\text{mol/L}$ NaHS in the presence of acidic pHe (Fig. 2C and D). We observed a significantly reduced OCR at 50 $\mu\text{mol/L}$ NaHS in both cancer cell lines. At lower sulfide concentration, the affinity of H_2S for the heme center of cytochrome C oxidase is too low to produce detectable inhibition of the enzyme (2), justifying the absence of OCR inhibition at lower NaHS concentrations. Hence, the trend toward an increased OCR in cells exposed to 1.5 $\mu\text{mol/L}$ NaHS corroborates that H_2S may also act as a mitochondrial electron donor when present in low concentration (26). At 100 $\mu\text{mol/L}$ NaHS, the same OCR inhibition as with rotenone, an inhibitor of mitochondrial respiration, was observed. To ensure that OCR inhibition was not due to cell mortality caused by the experimental conditions, viability assays were also performed. As shown in Supplementary Fig. S1A-S1D, no cell death was found.

**Figure 2.**

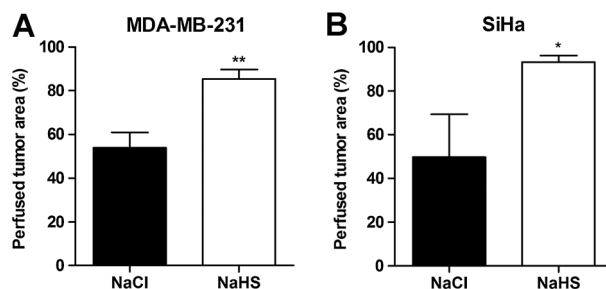
NaHS treatment decreases cancer cells OCR. OCR of viable MDA-MB-231 and SiHa cancer cells was measured *in vitro* using EPR (X-band) oximetry. A and B, cancer cells treated with 50 µmol/L NaHS or vehicle (NaCl 0.9%) in the presence of different pH values. C and D, cancer cells treated with increasing NaHS concentration or vehicle in the presence of pH = 6.5. Each bar represents mean OCR ± SEM. *, $P < 0.05$; **, $P < 0.01$; ***, $P < 0.001$; ns, not significant. Two-sided t test (A and B; $n = 3$) or ANOVA and Dunnett post-test (C and D; $n = 3$).

Blood perfusion was also investigated. Measurements were performed 15 minutes after NaHS injection using the Patent blue staining assay. This method, involving the injection of a dye in the systemic circulation of the mice, has previously been validated and compared with DCE-MRI (23). We observed that, as compared with vehicle-treated mice, the perfused area was increased in MDA-MB-231 (Fig. 3A) and SiHa (Fig. 3B) xenografts of NaHS-treated (100 µmol/kg) mice, indicating that increased perfusion also accounts for the improved tumor O₂ level following NaHS treatment.

NaHS radiosensitizes tumors by an "oxygen enhancement" effect

To investigate the therapeutic relevance of NaHS as a potential radiosensitizer, regrowth delay assays were performed in MDA-MB-231 tumors. Tumor growth curves are presented in Fig. 4A. Without irradiation, no difference in tumor growth was observed after a single i.p. administration of NaHS or vehicle. In irradiated groups, the regrowth delay to reach a 12-mm tumor diameter was 13.6 ± 2 days for irradiation + vehicle and 20.5 ± 3.5 for irradiation + NaHS, suggesting that NaHS administration 15 minutes before irradiation increased sensitivity of tumors by a factor of 1.5 (Fig. 4B). To highlight that NaHS radiosensitizes

tumor through an oxygen effect, we also used a group of mice receiving irradiation + NaHS whose legs were temporarily ligated to induce complete hypoxia at the time of irradiation. As the regrowth delay was similar to the irradiation + vehicle group

**Figure 3.**

NaHS injection increases blood perfusion. Perfusion of MDA-MB-231 (A) and SiHa (B) tumors was measured by Patent blue staining 15 minutes after NaHS (100 µmol/kg) or vehicle (NaCl 0.9%) i.p. injection. Each bar represents mean colored area ± SEM. *, $P < 0.05$; **, $P < 0.01$. Two-sided t test ($n = 4-5$ /group).

De Preter et al.

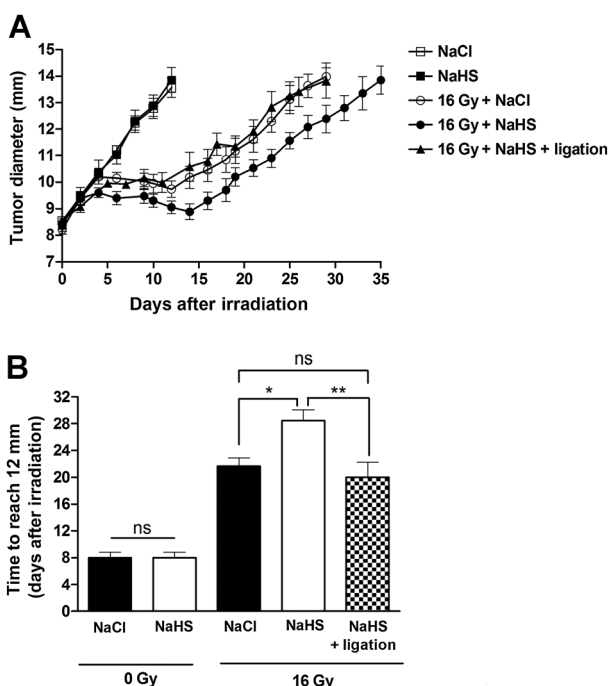


Figure 4. NaHS in combination with radiotherapy increases the radioresponse of MDA-MB-231 tumors. A, tumor growth curves of mice treated with NaHS (100 $\mu\text{mol/kg}$, ■) or vehicle (NaCl 0.9%, □) alone, 16 Gy of radiotherapy 15 minutes after NaHS (●) or vehicle (○) injection, and 16 Gy of radiotherapy 15 minutes after NaHS injection plus ligation at the time of irradiation (▲). Each point represents the mean tumor size \pm SEM. B, regrowth delay expressed as the time to reach a tumor size of 12 mm. *, $P < 0.05$; **, $P < 0.01$; ns, not significant. ANOVA and Bonferroni post-test ($n = 6/\text{group}$).

(Fig. 4B), this experiment showed that oxygen was necessary for NaHS to increase radioresponse.

Chronic NaHS injection alone is inactive to control tumor growth in mice

The potential inhibitory or stimulatory effect of the H_2S donor on tumor growth was also evaluated *in vivo*. Nude mice bearing MDA-MB-231 xenografts were daily i.p. injected with NaHS (100 $\mu\text{mol/kg/day}$) or vehicle (physiologic saline), and tumor diameter was measured until tumors reached 14 mm in diameter. Results showed that daily NaHS injection was inactive to control tumor growth, as no difference between NaHS-treated and vehicle-treated MDA-MB-231 tumor-bearing mice was found (Fig. 5A). Chronic NaHS injections seemed to have low incidence on the general condition of the mice, as no deterioration in body weight was observed as compared with vehicle-treated mice during the experiment (Fig. 5B).

Prolonged exposure to NaHS exhibits opposite effects on cancer cell proliferation depending on the extracellular pH

Some reports have already investigated the intrinsic anticancer properties of H_2S . Under different circumstances, H_2S acts as an inhibitor or as a promoter of proliferation for various cell types (27). It is currently hypothesized that conflictual conclusions arise from the manner in which cells are exposed to the treatment. We investigated whether pH could play a role in the

effects of NaHS on cancer cell proliferation. For the purpose, MDA-MB-231 cancer cells were incubated with 50 $\mu\text{mol/L}$ NaHS in alkaline (pH 7.4) or acidic (pH 6.5) media during 4 hours. Proliferation was assessed using quantitation of BrdU incorporated in the DNA of the cells during incubation. Our results showed opposite effects of NaHS depending on pH (Fig. 6A). In the presence of an alkaline pH, DNA synthesis in NaHS-treated cells increased, as compared with nontreated cells. In contrast, a decrease in DNA synthesis was induced by the H_2S donor when cells were incubated in an acidic medium. The decreased proliferation found in cells incubated at low pH was not associated with cell mortality (Supplementary Fig. S2). Further experiments were conducted to help understand the complex role of H_2S in cancer cell proliferation. We found that reactive oxygen species were not implicated in the pro- or antiproliferative effects of NaHS (Supplementary Fig. S3). We then asked whether a glycolytic switch occurred in the NaHS-treated cells. Indeed, enhanced glycolysis is known to confer advantages for cancer cell proliferation by providing reductive equivalents and glycolytic intermediates that fuel important biosynthetic reactions and promote cell expansion (28–30). We found a significant increase in glucose consumption (Fig. 6B) in NaHS-treated cells compared with nontreated cells in the alkaline condition, seemingly induced to maintain ATP homeostasis (Fig. 6C) in compensation to inhibition of the mitochondrial function. Supporting our findings, others have

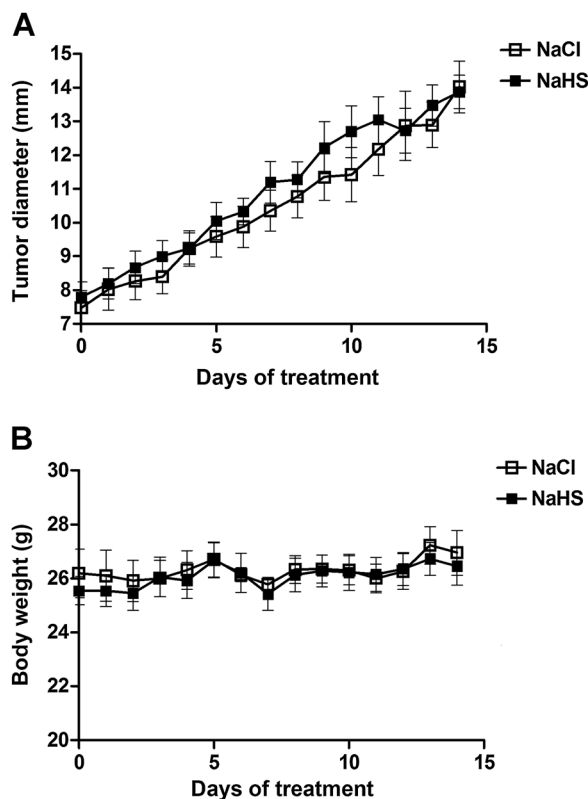


Figure 5. NaHS injected chronically is inactive on MDA-MB-231 tumor growth. Tumor growth (A) and body weight (B) of mice treated daily with NaHS (100 $\mu\text{mol/kg/day}$, ■) or vehicle (NaCl 0.9%, □). Each point represents mean \pm SEM ($n = 4/\text{group}$).

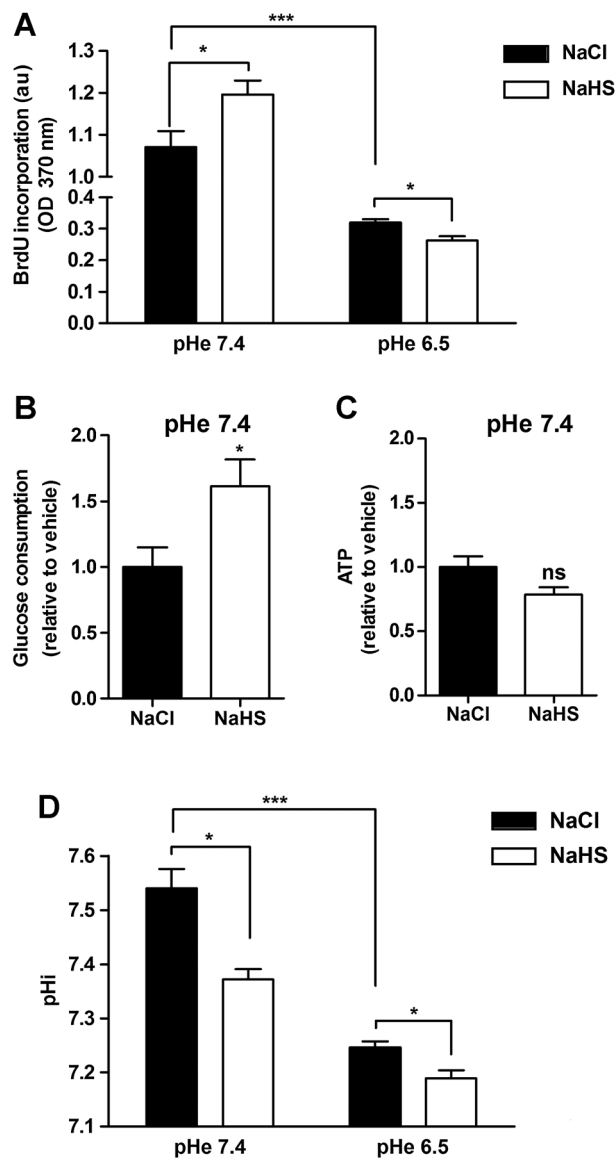


Figure 6. pH_e-dependent opposite effects of NaHS on MDA-MB-231 cancer cell proliferation. Cancer cells were incubated with 50 $\mu\text{mol/L}$ NaHS or vehicle (NaCl 0.9%) in the presence of different pH_e values during 4 hours. A, proliferation rates were analyzed by incorporation of a nucleotide analogue (BrdU) in the DNA of the cells during the incubation. B, glucose consumption was evaluated by measuring extracellular glucose concentrations before and after the 4-hour incubation in the presence of pH_e = 7.4. C, intracellular ATP level was quantified using a luciferase-based method after the 4-hour incubation in the presence of pH_e = 7.4. D, pH_i was measured using a fluorescent pH indicator. Each bar represents mean \pm SEM. *, $P < 0.05$; ***, $P < 0.001$; ns, not significant. Two-sided t test ($n \geq 3$).

also reported that a synthetic H₂S donor promotes an influx of glucose and triggers enhanced glycolysis in another human breast cancer cell line (31). We then analyzed the decreased proliferation induced by NaHS in the acidic condition. By noticing that low pH_e itself had profound impact on cancer cell proliferation, we questioned whether NaHS treatment was able to exacerbate the acidic stress experienced by cancer cells at

low pH_e. Indeed, it was recently evidenced that, besides its ability to enhance glycolysis, H₂S also impairs the activity of pH regulators in cancer cells, leading to the intracellular accumulation of acid and reduction of pH_i (31, 32). It is also known that pH_i must be kept in a narrow range, otherwise cell-cycle progression and biosynthetic processes are compromised (33). By measuring pH_i in MDA-MB-231 cancer cells, we observed that 4 hours of exposure to an acidic pH_e decreased pH_i and that an additional effect was found when NaHS was added (Fig. 6D).

Discussion

In this study, we showed that H₂S used as cotreatment to radiotherapy, but not as single treatment, provided beneficial effects for cancer therapy.

Clinical investigation has demonstrated that tumor hypoxia, arising from an imbalance between oxygen consumption and blood supply, is a major cause of resistance to radiotherapy. Therefore, selective targeting of cellular oxidative metabolism and/or tumor perfusion is challenging to radiosensitize tumors. For the first time, we report that administration of an H₂S donor (NaHS) before radiotherapy improves tumor oxygenation and radiosensitivity. Our results suggest that NaHS rapidly reduces tumor hypoxia by decreasing oxygen consumption by tumor cells and by increasing oxygen delivery by the tumor vasculature. Human cancer cells treated with NaHS exhibited a decreased OCR that was dose and pH-dependent. The potentiating effect of an acidic pH_e on OCR inhibition by NaHS is of particular interest, as hypoxic areas are generally associated with low pH due to cellular adaptations (28, 34) so that pH_e values as low as 6.5 have been observed in human tumors (35). Several mechanisms may be implicated in the enhanced inhibitory effect of NaHS on OCR at low pH_e. First, as H₂S dissociates to form HS⁻ + H⁺ ions with a pK_a close to 7, acidosis shifts the balance to the uncharged (H₂S) form, which is permeant to the cell membrane (25). Also, Nicholls and Kim have demonstrated that cytochrome C oxidase inhibition by H₂S is pH-dependent (K_i values ranging from 2.6 $\mu\text{mol/L}$ to 0.07 $\mu\text{mol/L}$ at pH of 8.05 to 6.28, respectively; ref. 36). We also observed that when incubated in the same experimental conditions, OCR inhibition by NaHS was more efficient in MDA-MB-231 cancer cells than in SiHa cancer cells. *In vivo*, a major increase in pO₂ was also found in MDA-MB-231 tumors following NaHS treatment. These different sensitivities may involve the capacity of cells to metabolize H₂S. It has been mathematically demonstrated (37) and experimentally validated (38) that targeting oxygen consumption was the most effective way to reduce tumor hypoxia. Therefore, the different cellular response observed in OCR experiments may account for the greater increased pO₂ found in MDA-MB-231 tumors following NaHS injection.

We also studied the effect of NaHS on tumor perfusion. At first glance, as H₂S induces vasorelaxation in numerous types of blood vessels (3), it would appear that a systemic administration of H₂S would lead to a negative response in tumor perfusion because of the so-called "steal effect" (39). However, our results showed that NaHS injected in the systemic circulation of the mice increased tumor perfusion in two tumor models. The fact that the vasoactive effects of H₂S are oxygen-dependent may play a beneficial role on the vascular response of hypoxic tumors. Indeed, both chronic and intermittent hypoxia increase the expression of K_{ATP} channels (40), the principal vascular target of

De Preter et al.

H₂S (3). Moreover, it has been reported that H₂S induces vasorelaxation much faster at below physiologic O₂ levels (41).

As we showed that NaHS increases tumor pO₂ by targeting both cancer cells metabolism and tumor perfusion, we then conducted radiosensitizing experiments in the MDA-MB-231 tumor model to test the therapeutic value of the use of NaHS in combination with radiotherapy. There was a significantly increased radioreponse of the tumors when irradiation was applied 15 minutes after NaHS injection, time at which tumor reoxygenation occurred. Confirming that the oxygen level is an important factor for radiosensitization by the H₂S donor, tumors that were clamped during the irradiation were not radiosensitized.

One area related to H₂S treatment for cancer that has already been studied is the effect on proliferation and survival. Changes in the expression of endogenous H₂S-producing enzymes (11) or exogenous administration of H₂S donors (8–10) suggest that H₂S controls tumor progression. Here, we studied the impact of pHe on the cellular response to prolonged exposure to NaHS. At pHe of 7.4, the H₂S donor increased glucose consumption. Enhanced glucose uptake was likely induced in cancer cells to compensate the ATP depletion due to the mitochondrial inhibition observed in these experimental conditions. Because enhanced glucose metabolism is known to promote cancer cell proliferation (28, 29), increased glycolysis by NaHS could potentially account for the increased DNA synthesis rate observed in our study. On the other hand, as H₂S also impaired pHi homeostasis, NaHS exhibited antiproliferative effects when cells were incubated at lower pHe. Taken together, our results emphasize how external factors influence cell response to H₂S.

The chronic injection of NaHS in mice did not provide significant effect on tumor growth, probably because of the microenvironmental heterogeneities characteristic of solid tumors, such as pH gradients. Using xenografts of leukemia cells in mice, others have evidenced the efficacy of a synthetic H₂S donor to restrain tumor growth (10). On the contrary, silencing of the H₂S-producing enzyme cystathionine-β-lyase decreased tumor growth (11). Further experiments with increasing dose of NaHS injected more repeatedly or intratumorally may highlight pro- or anticancer properties *in vivo*. Our experiment suggested a good tolerance of the mice to daily 100 μmol/kg NaHS administration, but more accurate monitoring of *in vivo* toxicity should be considered, especially in dose escalation experiments. Finally, as we showed that the antiproliferative effect of NaHS arises at low pH, more advanced tumors may be more sensitive to the treatment.

References

- Wang R. Hydrogen sulfide: the third gasotransmitter in biology and medicine. *Antioxid Redox Signal* 2010;12:1061–4.
- Collman JP, Ghosh S, Dey A, Decreau RA. Using a functional enzyme model to understand the chemistry behind hydrogen sulfide induced hibernation. *Proc Natl Acad Sci U S A* 2009;106:22090–5.
- Zhao W, Zhang J, Lu Y, Wang R. The vasorelaxant effect of H(2)S as a novel endogenous gaseous K(ATP) channel opener. *EMBO J* 2001;20:6008–16.
- Zhang Z, Huang H, Liu P, Tang C, Wang J. Hydrogen sulfide contributes to cardioprotection during ischemia-reperfusion injury by opening K ATP channels. *Can J Physiol Pharmacol* 2007;85:1248–53.
- Wang R. Physiological implications of hydrogen sulfide: a whiff exploration that blossomed. *Physiol Rev* 2012;92:791–896.
- Song ZJ, Ng MY, Lee Z-W, Dai W, Hagen T, Moore PK, et al. Hydrogen sulfide donors in research and drug development. *Med Chem Comm* 2014;5:557–70.
- Szabo C. Hydrogen sulphide and its therapeutic potential. *Nat Rev Drug Discov* 2007;6:917–35.
- Cai WJ, Wang MJ, Ju LH, Wang C, Zhu YC. Hydrogen sulfide induces human colon cancer cell proliferation: role of Akt, ERK and p21. *Cell Biol Int* 2010;34:565–72.
- Wu YC, Wang XJ, Yu L, Chan FK, Cheng AS, Yu J, et al. Hydrogen sulfide lowers proliferation and induces protective autophagy in colon epithelial cells. *PLoS One* 2012;7:e37572.
- Lee ZW, Zhou J, Chen CS, Zhao Y, Tan CH, Li L, et al. The slow-releasing hydrogen sulfide donor, GYY4137, exhibits novel anti-cancer effects in vitro and in vivo. *PLoS One* 2011;6:e21077.
- Szabo C, Hellmich MR. Endogenously produced hydrogen sulfide supports tumor cell growth and proliferation. *Cell Cycle* 2013;12:2915–6.
- Zhang J, Xie Y, Xu Y, Pan Y, Shao C. Hydrogen sulfide contributes to hypoxia-induced radioresistance on hepatoma cells. *J Radiat Res* 2011;52:622–8.

In conclusion, we report that NaHS, a fast H₂S-releasing donor, enhances radiotherapy efficacy by alleviating hypoxia in solid tumors. The good tolerance of the mice to chronic NaHS administration further pleads in favor of preclinical evaluation of the combination of H₂S donors to fractionated radiotherapy. When considering H₂S as single treatment for cancer, we report paradoxical effects of H₂S on cancer cell proliferation depending on external pH and no therapeutic benefits *in vivo*. Therefore, we suggest a new approach for the use of H₂S donors in combination therapy

Disclosure of Potential Conflicts of Interest

No potential conflicts of interest were disclosed.

Authors' Contributions

Conception and design: P. Sonveaux, B. Gallez

Development of methodology: G. De Preter, C. Deriemaeker, P. Danhier, L. Brisson, P. Sonveaux, B. Gallez

Acquisition of data (provided animals, acquired and managed patients, provided facilities, etc.): G. De Preter, C. Deriemaeker, P. Danhier, T.T. Cao Pham

Analysis and interpretation of data (e.g., statistical analysis, biostatistics, computational analysis): G. De Preter, C. Deriemaeker, P. Danhier, P. Sonveaux, B. Gallez

Writing, review, and/or revision of the manuscript: G. De Preter, P. Danhier, P. Sonveaux, B. Gallez

Administrative, technical, or material support (i.e., reporting or organizing data, constructing databases): G. De Preter

Study supervision: V. Grégoire, B.F. Jordan, P. Sonveaux, B. Gallez

Grant Support

This study was supported by grants from the Fonds National de la Recherche Scientifique (F.R.S.-FNRS, PDR T.0107.13; to B. Gallez), the Fonds Joseph Maisin (to B.F. Jordan and B. Gallez), the Action de Recherches Concertées ARC 14/19-058 (to V. Grégoire, B.F. Jordan, P. Sonveaux, and B. Gallez), and a Starting Grant from the European Research Council (ERC No. 243188 TUMETABO to P. Sonveaux). G. De Preter and T.T. Cao-Pham are Télévie PhD Fellows, P. Danhier is a Postdoctoral Télévie Fellow, B.F. Jordan and P. Sonveaux are Research Associates of the F.R.S.-FNRS.

The costs of publication of this article were defrayed in part by the payment of page charges. This article must therefore be hereby marked *advertisement* in accordance with 18 U.S.C. Section 1734 solely to indicate this fact.

Received August 20, 2015; revised November 3, 2015; accepted November 5, 2015; published OnlineFirst December 18, 2015.

13. Jordan BF, Gregoire V, Demeure RJ, Sonveaux P, Feron O, O'Hara J, et al. Insulin increases the sensitivity of tumors to irradiation: involvement of an increase in tumor oxygenation mediated by a nitric oxide-dependent decrease of the tumor cells oxygen consumption. *Cancer Res* 2002;62:3555–61.
14. Jordan BF, Sonveaux P, Feron O, Gregoire V, Beghein N, Gallez B. Nitric oxide-mediated increase in tumor blood flow and oxygenation of tumors implanted in muscles stimulated by electric pulses. *Int J Radiat Oncol Biol Phys* 2003;55:1066–73.
15. Sonveaux P, Jordan BF, Gallez B, Feron O. Nitric oxide delivery to cancer: why and how? *Eur J Cancer* 2009;45:1352–69.
16. Rockwell S, Dobrucki IT, Kim EY, Marrison ST, Vu VT. Hypoxia and radiation therapy: past history, ongoing research, and future promise. *Curr Mol Med* 2009;9:442–58.
17. Harada H. How can we overcome tumor hypoxia in radiation therapy? *J Radiat Res* 2011;52:545–56.
18. Tatum JL, Kelloff GJ, Gillies RJ, Arbeit JM, Brown JM, Chao KS, et al. Hypoxia: importance in tumor biology, noninvasive measurement by imaging, and value of its measurement in the management of cancer therapy. *Int J Radiat Biol* 2006;82:699–757.
19. Thomlinson RH, Gray LH. The histological structure of some human lung cancers and the possible implications for radiotherapy. *Br J Cancer* 1955;9:539–49.
20. James PE, Jackson SK, Grinberg OY, Swartz HM. The effects of endotoxin on oxygen consumption of various cell types in vitro: an EPR oximetry study. *Free Radic Biol Med* 1995;18:641–7.
21. Gallez B, Baudalet C, Jordan BF. Assessment of tumor oxygenation by electron paramagnetic resonance: principles and applications. *NMR Biomed* 2004;17:240–62.
22. Gallez B, Jordan BF, Baudalet C, Misson PD. Pharmacological modifications of the partial pressure of oxygen in murine tumors: evaluation using in vivo EPR oximetry. *Magn Reson Med* 1999;42:627–30.
23. Ansaux R, Baudalet C, Jordan BF, Beghein N, Sonveaux P, De Wever J, et al. Thalidomide radiosensitizes tumors through early changes in the tumor microenvironment. *Clin Cancer Res* 2005;11:743–50.
24. Wang MJ, Cai WJ, Li N, Ding YJ, Chen Y, Zhu YC. The hydrogen sulfide donor NaHS promotes angiogenesis in a rat model of hind limb ischemia. *Antioxid Redox Signal* 2010;12:1065–77.
25. Nagy P, Palinkas Z, Nagy A, Budai B, Toth I, Vasas A. Chemical aspects of hydrogen sulfide measurements in physiological samples. *Biochim Biophys Acta* 2014;1840:876–91.
26. Szabo C, Ransy C, Modis K, Andriamihaja M, Murghes B, Coletta C, et al. Regulation of mitochondrial bioenergetic function by hydrogen sulfide. Part I. Biochemical and physiological mechanisms. *Br J Pharmacol* 2014;171:2099–122.
27. Yang G. Hydrogen sulfide in cell survival: a double-edged sword. *Expert Rev Clin Pharmacol* 2011;4:33–47.
28. Gatenby RA, Gillies RJ. Why do cancers have high aerobic glycolysis? *Nat Rev Cancer* 2004;4:891–9.
29. Lunt SY, Vander Heiden MG. Aerobic glycolysis: meeting the metabolic requirements of cell proliferation. *Annu Rev Cell Dev Biol* 2011;27:441–64.
30. Porporato PE, Dhup S, Dadhich RK, Copetti T, Sonveaux P. Anticancer targets in the glycolytic metabolism of tumors: a comprehensive review. *Front Pharmacol* 2011;2:49.
31. Lee ZW, Teo XY, Tay EY, Tan CH, Hagen T, Moore PK, et al. Utilizing hydrogen sulfide as a novel anti-cancer agent by targeting cancer glycolysis and pH imbalance. *Br J Pharmacol* 2014;171:4322–36.
32. Hu LF, Li Y, Neo KL, Yong QC, Lee SW, Tan BK, et al. Hydrogen sulfide regulates Na⁺/H⁺ exchanger activity via stimulation of phosphoinositide 3-kinase/Akt and protein kinase C pathways. *J Pharmacol Exp Ther* 2011;339:726–35.
33. Madhus IH. Regulation of intracellular pH in eukaryotic cells. *Biochem J* 1988;250:1–8.
34. Chiche J, Brahimi-Horn MC, Pouyssegur J. Tumour hypoxia induces a metabolic shift causing acidosis: a common feature in cancer. *J Cell Mol Med* 2010;14:771–94.
35. Gerweck LE, Seetharaman K. Cellular pH gradient in tumor versus normal tissue: potential exploitation for the treatment of cancer. *Cancer Res* 1996;56:1194–8.
36. Nicholls P, Kim JK. Sulphide as an inhibitor and electron donor for the cytochrome c oxidase system. *Can J Biochem* 1982;60:613–23.
37. Secomb TW, Hsu R, Ong ET, Gross JF, Dewhirst MW. Analysis of the effects of oxygen supply and demand on hypoxic fraction in tumors. *Acta Oncol* 1995;34:313–6.
38. Diepart C, Karroum O, Magat J, Feron O, Verrax J, Calderon PB, et al. Arsenic trioxide treatment decreases the oxygen consumption rate of tumor cells and radiosensitizes solid tumors. *Cancer Res* 2012;72:482–90.
39. Zlotecki RA, Baxter LT, Boucher Y, Jain RK. Pharmacologic modification of tumor blood flow and interstitial fluid pressure in a human tumor xenograft: network analysis and mechanistic interpretation. *Microvasc Res* 1995;50:429–43.
40. Shimoda LA, Polak J. Hypoxia. 4. Hypoxia and ion channel function. *Am J Physiol Cell Physiol* 2011;300:C951–67.
41. Koenitzer JR, Isbell TS, Patel HD, Benavides GA, Dickinson DA, Patel RP, et al. Hydrogen sulfide mediates vasoactivity in an O₂-dependent manner. *Am J Physiol Heart Circ Physiol* 2007;292:H1953–60.

Molecular Cancer Therapeutics

A Fast Hydrogen Sulfide–Releasing Donor Increases the Tumor Response to Radiotherapy

Géraldine De Preter, Caroline Deriemaeker, Pierre Danhier, et al.

Mol Cancer Ther 2016;15:154-161. Published OnlineFirst December 18, 2015.

Updated version Access the most recent version of this article at:
doi:[10.1158/1535-7163.MCT-15-0691-T](https://doi.org/10.1158/1535-7163.MCT-15-0691-T)

Supplementary Material Access the most recent supplemental material at:
<http://mct.aacrjournals.org/content/suppl/2015/12/18/1535-7163.MCT-15-0691-T.DC1>

Cited articles This article cites 41 articles, 8 of which you can access for free at:
<http://mct.aacrjournals.org/content/15/1/154.full#ref-list-1>

E-mail alerts [Sign up to receive free email-alerts](#) related to this article or journal.

Reprints and Subscriptions To order reprints of this article or to subscribe to the journal, contact the AACR Publications Department at pubs@aacr.org.

Permissions To request permission to re-use all or part of this article, use this link
<http://mct.aacrjournals.org/content/15/1/154>.
Click on "Request Permissions" which will take you to the Copyright Clearance Center's (CCC) Rightslink site.